

Large Photoluminescence Enhancement by an Out-of-Plane Magnetic Field in Exfoliated WS₂ Flakes

Sibai Sun(孙思白)^{1,2}, Jianchen Dang(党剑臣)^{1,2}, Xin Xie(谢昕)^{1,2}, Yang Yu(于洋)^{1,2}, Longlong Yang(杨龙龙)^{1,2}, Shan Xiao(肖姗)^{1,2}, Shiyao Wu(武诗瑶)^{1,2}, Kai Peng(彭凯)^{1,2}, Feilong Song(宋飞龙)^{1,2}, Yunuan Wang(王玉暖)^{1,3}, Jingnan Yang(杨静南)^{1,2}, Chenjiang Qian(钱琛江)^{1,2}, Zhanchun Zuo(左战春)^{1,2}, and Xiulai Xu(许秀来)^{1,2,4*}

¹Beijing National Laboratory for Condensed Matter Physics, Institute of Physics, Chinese Academy of Sciences, Beijing 100190, China

²CAS Center for Excellence in Topological Quantum Computation and School of Physical Sciences, University of Chinese Academy of Sciences, Beijing 100049, China

³Key Laboratory of Luminescence and Optical Information (Ministry of Education), Beijing Jiaotong University, Beijing 100044, China

⁴Songshan Lake Materials Laboratory, Dongguan 523808, China

(Received 3 May 2020; accepted 4 June 2020; published online 28 July 2020)

We report an out-of-plane magnetic field induced large photoluminescence enhancement in WS₂ flakes at 4 K, in contrast to the photoluminescence enhancement provided by an in-plane field in general. Two mechanisms for the enhancement are proposed. One is a larger overlap of the electron and hole caused by the magnetic field induced confinement. The other is that the energy difference between Λ and K valleys is reduced by magnetic field, and thus enhancing the corresponding indirect-transition trions. Meanwhile, the Landé g factor of the trion is measured to be -0.8 , whose absolute value is much smaller than normal exciton, which is around $|-4|$. A model for the trion g factor is presented, confirming that the smaller absolute value of the Landé g factor is a behavior of this Λ - K trion. By extending the valley space, we believe this work provides a further understanding of the valleytronics in monolayer transition metal dichalcogenides.

PACS: 78.67.-n, 78.55.-m

DOI: 10.1088/0256-307X/37/8/087801

Recently optical properties with valley features of transition metal dichalcogenides (TMDs) have been investigated intensively.^[1–5] Especially, the magneto-optical properties have raised a great deal of attention since magneto-photoluminescence spectroscopy is a promising tool to investigate spin and valley properties of excitons.^[6–10] Normally, the valley and spin information is locked by the selection rule. By applying a magnetic field, the degeneracy of the spin is lifted, and the valley information will change accordingly. Due to the fact that the spin-orbit couplings of a conduction band and valence band have opposite signs,^[11,12] the lower energy state does not emit photons because of the selection rule for darkish materials.^[13] In-plane magnetic field induces tunneling between two spin statuses, and thus unlocking the restriction between spin and valley information, making the dark excitons bright. Therefore, the photoluminescence (PL) can be enhanced by applying an in-plane magnetic field in monolayer darkish

materials.^[13,14] However, different from the in-plane magnetic field, out-of-plane magnetic field-induced PL enhancement in monolayer TMDs has yet to be explored.

In addition to the external field modulating the PL, the valley features may also affect the PL intensity. Recently, the intervalley excitons including K , Λ valleys (middle point between Γ and K , sometimes also called Q valley^[15]) in the conduction band and K , Γ valleys in the valence band have been investigated.^[16] The properties of these valleys can be quite different from K valleys, such as orbital magnetic momenta, spin status of eigenstates, energy shifts by strain and effective masses of carriers.^[17–19] The differences provide an opportunity to open a new field of information processing considering the valley freedom.

In this work, we report an observation of strong PL enhancement by the out-of-plane magnetic field at cryogenic temperature. Two mechanisms for the en-

Supported by the National Natural Science Foundation of China (Grants Nos. 11934019, 61675228, 11721404, 51761145104 and 11874419), the Strategic Priority Research Program, the Instrument Developing Project and the Interdisciplinary Innovation Team of the Chinese Academy of Sciences (Grant Nos. XDB28000000 and YJKYYQ20180036), and the Key Research and Development Program of Guangdong Province (Grant No. 2018B030329001).

*Corresponding author. Email: xlxu@iphy.ac.cn

© 2020 Chinese Physical Society and IOP Publishing Ltd

hancement are provided. One is the increase of wavefunction overlapping between electron and hole. The other is the enhanced indirect transitions between K and Λ valleys in WS_2 flakes, which is a result of the decrease of the energy difference of K and Λ valleys in the out-of-plane magnetic field, accompanied with a small absolute Landé g factor value.

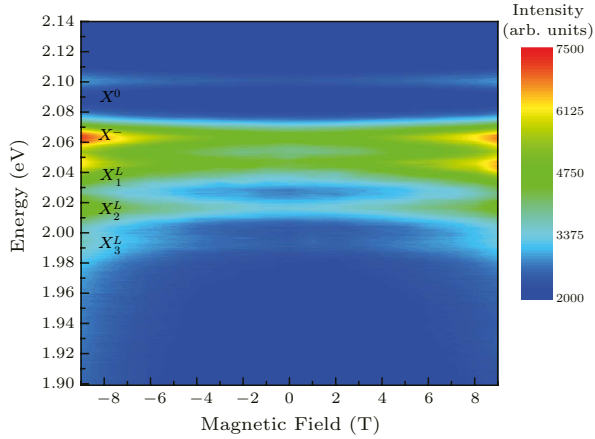


Fig. 1. Contour plot of PL spectra from a WS_2 flake with a vertical magnetic field from -9 T to 9 T at 4.2 K . When the magnetic field increases, the neutral exciton peak (X^0), trion peak (X^-) and defect-bound excitons ($X_{1,2,3}^L$) are enhanced significantly.

Experimental Results and Discussions. The WS_2 flakes are exfoliated from bulk materials and transferred to a Si/SiO_2 substrate as shown in the inset of Fig. 2(a). The PL spectra from WS_2 flake at different magnetic fields are shown in Fig. 1 at 4.2 K with an excitation laser at 532 nm . The exciton peak (marked as X^0) at 2.10 eV , the negative trion peaks (marked as X^-) at 2.06 eV and defect-bound excitons (marked as $X_j^L, j = 1, 2, 3$) at lower energy are identified.^[20] The charged trion in monolayer WS_2 has been confirmed to be negative by electric tuning.^[21,22] By measuring the variation of PL intensity logarithm with different pumping powers, the contribution of bi-exciton is excluded.^[23] Since the direction of the magnetic field is out-of-plane, the contribution of the dark exciton is excluded.^[24] It can be seen that the intensities of PL peaks increase with increasing magnetic field. In order to obtain the intensity increase in detail, the PL spectra are fitted with a multi-peak non-linear least-square curve-fitting python package in the Lorentz shape as shown in Fig. 2(a). When the magnetic field is increased to 9 T , the integration PL intensities of the neutral exciton (X^0), trion peak (X^-) and defect-bound excitons ($X_{1,2,3}^L$) are enhanced by 47% , 70% , 67% , 93% and 174% , respectively, as shown in Fig. 2(b). The origin of the broad peak at 1.9 eV is still unclear, which does not show a clear enhancement with magnetic field.

The enhancement of emission with an applied magnetic field has been reported in other low di-

mensional semiconductor materials, such as quantum dot and quantum well systems in III-V compound semiconductors.^[25–27] The magnetic field transforms the wavefunction of electron and hole and reduces wavefunction extension. Due to the large difference of effective masses of electrons and holes,^[28] or the difference of band structures in heterostructure-like core-shell quantum dots,^[29] the electrons and holes are spatially separated. The wavefunction extension modulation could increase the overlap of their wavefunction distribution, then influence the recombination rate, and thus resulting in a PL intensity enhancement.

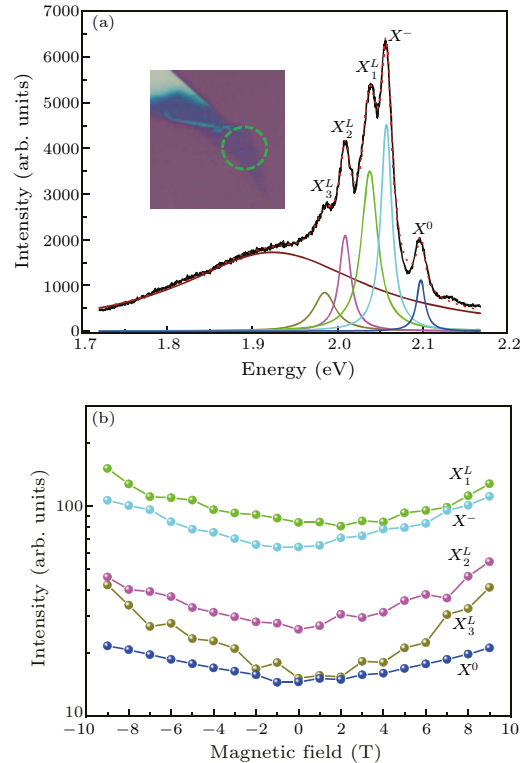


Fig. 2. (a) Photoluminescence spectrum from the WS_2 flake with magnetic field of 9 T at 4.2 K . The black line is the PL spectrum, and the color lines are the multi-peak fitted curves. The optical microscope image is shown in the inset. (b) Peak integration intensities of X^0 , X^- and $X_{1,2,3}^L$ in different magnetic fields. At 9 T , the integration PL intensities of the neutral exciton (X^0), trion peak (X^-) and defect-bound excitons ($X_{1,2,3}^L$) are enhanced by 47% , 70% , 67% , 93% and 174% , respectively.

Generally, in the WS_2 , there are neither such a large effective mass difference, nor spacial difference like heterostructure. However, due to impurities or defects, a spacial difference will also be induced. For example, impurities capture carriers and form-charged centers. Then excitons interact with these charged centers, leading to wavefunction radius modification by Coulomb interaction. The opposite charges between the electron and hole make the modifications opposite, and thus induce the spacial difference. For Wannier-like excitons, the typical length scale of the

ground state is $a = \frac{\epsilon_r m_0}{m_{\text{eff}}} a_B$,^[30] where ϵ_r is the relative dielectric constant, m_0 is the electron mass in vacuum, m_{eff} is the effective reduced mass for the exciton, and a_B is the Bohr radius of the hydrogen atom. For WS₂, the $m_{\text{eff}} \approx 0.5m_0$ for both electrons and holes, and relative dielectric constant $\epsilon_r \approx 10$,^[31] therefore $a \approx 1$ nm. The length scale of carriers with magnetic field can be expressed by gyroradius $r(B) = \sqrt{\frac{\hbar}{eB}}$. With magnetic field of 9 T, it is around 8 nm. The influence of magnetic field cannot be neglected for defect-bound exciton. When magnetic field is applied, the wavefunction shape of trapped carriers will be shrunk, making electrons and holes more likely to recombine.

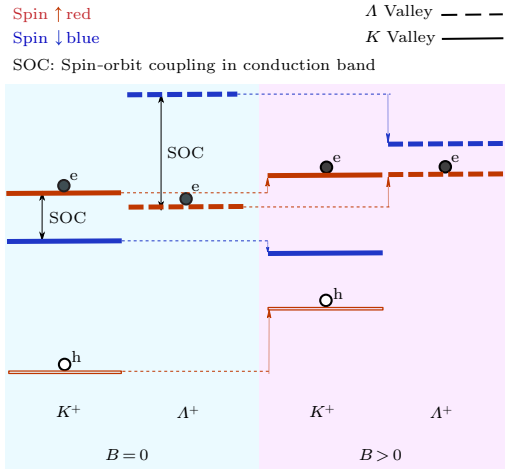


Fig. 3. Band structures without (left, sky blue background) and with a magnetic field (right, violet background). Red lines represent bands whose spin eigenstate are up, and blue lines for down. The A - K trion contains a hole and an electron in K valley, and another electron in the A valley. Due to the difference of orbital terms between the A valley and K valley, the band shifts differently with magnetic field.

Meanwhile, the PL enhancement could be introduced by the reduction of the energy difference between the K and A valleys. As shown in Fig. 3, without magnetic field, the spin-up energy level of A^+ valley is lower than that of K^+ , and the spin-down energy level of the A^- valley is lower than K^- . Here, we take spin-up situation as an example. Once magnetic field is applied on these flakes, the A valley shifting will be larger than the K valley shifting, which will be explained later in Eq. (6). As a result, the energy difference between K and A is reduced, as shown in Fig. 3. Thus the intervalley scattering between the A electron and K electron occurs more frequently, which can be derived from models of Raman spectrum analysis.^[32] This scattering thus influences the occupation status of electrons, making the PL more bright. If the magnetic field is positive, the σ^+ component will be enhanced. If it is negative, the σ^- component will be enhanced. Therefore, related PL peaks are enhanced.

The influence of A valley not only affects the PL intensity, but also the Landé g factors. The g factors for conduction band and valence band at each valley are expressed as

$$g_b^{V^\pm, s} = \frac{E_b^{V^\pm, s}(B) - E_b^{V^\pm, s}(0)}{\mu_B B}, \quad (1)$$

where B is the out-of-plane magnetic field, $b = \{c, v\}$ denotes conduction and valence band respectively, $V^\pm = \{K^+, K^-, A^+, A^-\}$ denotes the valleys, and $s = \{\uparrow, \downarrow\}$ denotes spin. For normal excitons, the Landé g factor can then be expressed by $g = g_c^{V, \uparrow} - g_v^{V, \uparrow} - g_c^{V, \downarrow} + g_v^{V, \downarrow}$. The linear energy level shift caused by magnetic field can be contributed by three parts: spin, orbital and valley components:^[33–36] $g_b^{V, s} = g_b^{V, s}(\text{spin}) + g_b^{V, s}(\text{orbit}) + g_b^{V, s}(\text{valley})$. For neutral exciton in TMDs, the spins of electron and hole are in the same direction, the spin term is zero, i.e., $g_c^{V, s}(\text{spin}) - g_v^{V, s}(\text{spin}) = (\pm\frac{1}{2}) - (\pm\frac{1}{2}) = 0$.^[37] The orbital terms are mainly from the angular momentum azimuthal component of the electron state around the transition metal atom, $g_b^{V, s}(\text{orbit}) = \langle \hat{L}_z \rangle / \hbar$. For the conduction band at the K point, the electron mainly possesses $|K_c^\pm\rangle = |d_{z^2}\rangle$ orbit and thus the azimuthal component is $\langle K_c^\pm | \hat{L}_z | K_c^\pm \rangle = 0$. For the valence band at K point, the state mainly possesses $|K_v^\pm\rangle = \frac{1}{\sqrt{2}}(|d_{x^2-y^2}\rangle \pm i|d_{xy}\rangle)$ orbit and the azimuthal component is $\langle K_v^\pm | \hat{L}_z | K_v^\pm \rangle = \pm 2\hbar$.^[1] Therefore the orbital term is $g(\text{orbit}) = (0 - (+2)) - (0 - (-2)) = -4$. The valley term is proportional to the inverse of effective mass. For the conduction band it is $g_c^{V^\pm, s}(\text{valley}) = \pm m_0 / m_e^V$, and for the valence band it is $g_v^{V^\pm, s}(\text{valley}) = \mp m_0 / m_h^V$, where m_e^V and m_h^V are the effective masses of the electron and hole at the V valley respectively. Thus the valley term is $g(\text{valley}) = (m_0 / m_e^V - m_0 / m_h^V) - [(-m_0 / m_e^V) - (-m_0 / m_h^V)] = 2(m_0 / m_e^V - m_0 / m_h^V)$.^[38] In total, $g_{X^0} = -4 + 2(m_0 / m_e^K - m_0 / m_h^K)$. Because the effective masses of m_e and m_h are similar in WS₂.^[19] Therefore, the g factor of the exciton is around -4 , which has been confirmed experimentally before.^[39,40]

For negative trion, there are two electrons e_1, e_2 and one hole h , where e_1 at V_1^\pm valley with spin s_1^\pm , e_2 at V_2^\pm valley with spin s_2^\pm , and h at V_h^\pm valley. Due to the large spin-orbit coupling (SOC) in the valence band, excitons are clearly separated into A excitons and B excitons by energy difference. Here \pm denotes the hole spin direction of A excitons. If we neglect the influence of binding energy variation by magnetic field, only focus on the Zeeman effect, then the g factor can be expressed as $g = g_c^{V_j^+, s_j^+} - g_v^{V_h^+, \uparrow} - g_c^{V_j^-, s_j^-} + g_v^{V_h^-, \downarrow}$, where $j = \{1, 2\}$ is the electron index whose energy level is lower. Since there are two electrons, the excess electron of negative trion can fall in other valleys without

violating the momentum conservation rule. If this excessive electron possesses the same \mathbf{k} vector but different spins, then the trion will be a singlet trion; if this extra electron falls in the opposite \mathbf{k} vectors but same spin, then the trion is a triplet trion. For the singlet, $V_1^\pm = K^\pm$, $V_2^\pm = K^\pm$, $V_h^\pm = K^\pm$, $E(e_1) > E(e_2)$, $s_2^\pm = \mp\hbar/2$,

$$\begin{aligned} g(\mathbf{X}_{\text{singlet}}^-) &= g_c^{K^+, \downarrow} - g_v^{K^+, \uparrow} - g_c^{K^-, \uparrow} + g_v^{K^-, \downarrow} \\ &= [(-1/2) - (+1/2) - (+1/2) + (-1/2)] + \\ &\quad + [0 - (+2) - 0 + (-2)] + \\ &\quad + \left[\left(+\frac{m_0}{m_e^K} \right) - \left(+\frac{m_0}{m_h^K} \right) - \left(-\frac{m_0}{m_e^K} \right) + \left(-\frac{m_0}{m_h^K} \right) \right] \\ &= -6 + 2(m_0/m_e^K - m_0/m_h^K) \approx -6. \end{aligned} \quad (2)$$

For the triplet, $V_1^\pm = K^\pm$, $V_2^\pm = K^\mp$, $V_h^\pm = K^\pm$, $E(e_1) > E(e_2)$, $s_2^\pm = \pm\hbar/2$,

$$\begin{aligned} g(\mathbf{X}_{\text{triplet}}^-) &= g_c^{K^-, \uparrow} - g_v^{K^+, \uparrow} - g_c^{K^+, \downarrow} + g_v^{K^-, \downarrow} \\ &= [(+1/2) - (+1/2) - (-1/2) + (-1/2)] + \\ &\quad + [0 - (+2) - 0 + (-2)] + \\ &\quad + \left[\left(-\frac{m_0}{m_e^K} \right) - \left(+\frac{m_0}{m_h^K} \right) - \left(+\frac{m_0}{m_e^K} \right) + \left(-\frac{m_0}{m_h^K} \right) \right] \\ &= -4 - 2(m_0/m_e^K + m_0/m_h^K) \ll -4. \end{aligned} \quad (3)$$

This is close to the experimental data. For example, in WSe₂, the g factor is around $g = -5.3$ of singlet, and -10.5 of triplet.^[41]

The A - K trions, whose extra electron falls in A valley instead of K , have different orbital momentum from K - K trions, leading to different g factors. The electron state of conduction band is no more constituted of $|d_{z^2}\rangle$ orbit, but is a superposition of several states. To investigate the g factor of the A - K trion, we estimated the orbital projections at A valley, along with the band structure of monolayer WS₂. The *ab-initio* calculation is based on the density functional theory. The projector augmented wave method^[42] is used together with local density approximation. Four empty cell layers are filled between material layers to prevent interlayer interactions. The positions of atoms are initialized with structure data from Materials Project mp-224.^[43] Before the electron density wave calculation, an ionic relaxation is executed to ensure the structure stable. The SOC is not considered in this calculation, since its influence to projection amplitudes is a minor term. The main influence of SOC is lifting the degeneracy of spins.

The result of projections on the orbital states around tungsten atoms are 1.6% of s , 0.9% of p_x , 0.7% of p_y , 43.1% of $d_{x^2-y^2}$, 32.5% of d_{xy} , 21.1% of d_{z^2} , and 0 of else. For any state $|\psi\rangle$, if we have $\langle p_x|\psi\rangle = A_x \exp(i\phi_x)$ and $\langle p_y|\psi\rangle = A_y \exp(i\phi_y)$, then $|\langle p_+|\psi\rangle|^2 - |\langle p_-|\psi\rangle|^2 = 2A_x A_y \sin(\phi_y - \phi_x)$, where $|p_\pm\rangle = \frac{1}{\sqrt{2}}(|p_x\rangle \pm i|p_y\rangle)$. The phase difference will

change to $\pm\frac{\pi}{2}$ when degeneracy is broken by the magnet field or SOC. The amplitudes of components thus are

$$\begin{aligned} |\langle p_+|\psi_\pm\rangle|^2 - |\langle p_-|\psi_\pm\rangle|^2 &= \pm 2|\langle p_x|\psi_\pm\rangle||\langle p_y|\psi_\pm\rangle| \\ &= \pm 2\sqrt{0.9\% \times 0.7\%} = \pm 0.016, \\ |\langle d_{(x+iy)^2}|\psi_\pm\rangle|^2 - |\langle d_{(x-iy)^2}|\psi_\pm\rangle|^2 \\ &= \pm 2|\langle d_{x^2-y^2}|\psi_\pm\rangle||\langle d_{xy}|\psi_\pm\rangle| \\ &= \pm 2\sqrt{43.1\% \times 32.5\%} = \pm 0.7495, \\ |\langle d_{(x\pm iy)z}|\psi_\pm\rangle|^2 &= 0, \end{aligned} \quad (4)$$

where $|\psi_\pm\rangle$ is the state of A^\pm valley. Therefore the expected orbital angular momentum component in z direction around the tungsten atom should be

$$\begin{aligned} \langle \hat{L}_z \rangle &= 2\hbar|\langle d_{(x+iy)^2}|\psi\rangle|^2 - 2\hbar|\langle d_{(x-iy)^2}|\psi\rangle|^2 \\ &\quad + \hbar|\langle d_{(x+iy)z}|\psi\rangle|^2 - \hbar|\langle d_{(x-iy)z}|\psi\rangle|^2 + 0\hbar|\langle d_{z^2}|\psi\rangle|^2 \\ &\quad + \hbar|\langle p_+|\psi\rangle|^2 - \hbar|\langle p_-|\psi\rangle|^2 + 0\hbar|\langle s|\psi\rangle|^2 \\ &= \pm \left(2 \times 0.7495 + 0 + 0 + 0.016 + 0 \right) \hbar \\ &= \pm 1.515\hbar. \end{aligned} \quad (5)$$

Thus the conduction band energy shift of A valley is larger than K valley,

$$g_c^{A^+, \uparrow} = \frac{1}{2} + 1.515 + \frac{m_0}{m_e^A} > \frac{1}{2} + 0 + \frac{m_0}{m_e^K} = g_c^{K^+, \uparrow}. \quad (6)$$

Therefore the energy difference between A valley and K valley is reduced by magnetic field, which leads to the PL enhancement.

As for the g factor of A - K trion: $V_1^\pm = K^\pm$, $V_2^\pm = A^\pm$, $V_h^\pm = K^\pm$, $E(e_1) > E(e_2)$, $s_2^\pm = \pm\hbar/2$,

$$\begin{aligned} g(\mathbf{X}_{A-K}^-) &= g_c^{A^+, \uparrow} - g_v^{K^+, \uparrow} - g_c^{A^-, \downarrow} + g_v^{K^-, \downarrow} \\ &= [(+1/2) - (+1/2) - (-1/2) + (-1/2)] + \\ &\quad + [(+1.515) - (+2) - (-1.515) + (-2)] + \\ &\quad + \left[\left(+\frac{m_0}{m_e^A} \right) - \left(+\frac{m_0}{m_h^K} \right) - \left(-\frac{m_0}{m_e^A} \right) + \left(-\frac{m_0}{m_h^K} \right) \right] \\ &= -0.970 - 2(m_0/m_e^A - m_0/m_h^K). \end{aligned} \quad (7)$$

Since the effective masses of the electron and hole are similar, we neglect the g_{valley} in the same way as K - K trion. Therefore $g \approx -0.97$, whose absolute value is extraordinarily small.

In order to obtain the Landé g factor of the exciton states experimentally, we measured σ^+ and σ^- components of the PL spectra at different magnetic fields. The normalized spectra for 9 T, 0 T and -9 T are shown in Fig. 4(a). The red curves are σ^+ polarization and the blue curves are σ^- polarization. The peak centers are extracted by multi-peak non-linear least-squares curve-fitting python package from spectra. The g factor is extracted by linear regression of the peak centers. The measured g factor of X^0 is -3.08 , close to the theoretical value (around

–4).^[39,40] The measured g factors of $X_{1,2,3}^L$ are -4.9 , -7.2 and -10.2 , respectively, consistent with the reported values in TMDs.^[8] So far, the g factors of defect-bound excitons vary in a wide range from -6 to -16 , which has been reported in TMDs.^[44–46] Our results for defect related peaks fall in this range. Surprisingly, the measured g factor of X^- is -0.8 , whose absolute value is much smaller than the above values as shown in Fig. 4(c). The small absolute value is close to our calculation result $|-0.97|$, which confirms our assumption that the trion is an indirect transition between Λ and K valleys. With the assistance of Λ – K trions, the PL intensity can be enhanced.

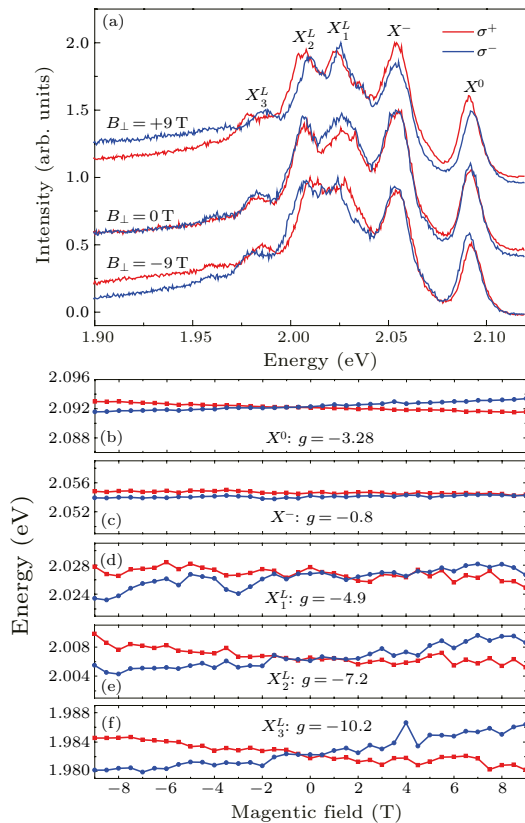


Fig. 4. (a) The normalized spectra for 9 T, 0 T and -9 T. (b)–(f) Peak centers of (b) X^0 , (c) X^- and (d)–(f) $X_{1,2,3}^L$ for σ^+ (red) and σ^- (blue) polarizations. The g factor of X^- is -0.8 , whose absolute value is smaller than other excitons, while the g factors of X^0 and $X_{1,2,3}^L$ are consistent with the previous reports.^[8,39,40]

In conclusion, a magnetic field-induced large PL enhancement of WS_2 in a cryogenic environment is reported. Two mechanisms have been discussed to explain the enhancement qualitatively. One is attributed to the magnetic field induced wavefunction confinement causing a larger overlap of electron and hole wavefunction extension. The other is related to an indirect-transition trion between Λ and K valleys. According to the model considered, the Λ – K trion has a smaller absolute value of g factor than K – K trions, which is confirmed experimentally. We believe this

work will extend valleytronics with different valleys in monolayer TMDs in future.

References

- [1] Xiao D, Liu G B, Feng W, Xu X and Yao W 2012 *Phys. Rev. Lett.* **108** 196802
- [2] Mak K F, Lee C, Hone J, Shan J and Heinz T F 2010 *Phys. Rev. Lett.* **105** 136805
- [3] Splendiani A, Sun L, Zhang Y, Li T, Kim J, Chim C Y, Galli G and Wang F 2010 *Nano Lett.* **10** 1271
- [4] Zhao W, Ghorannevis Z, Chu L, Toh M, Kloc C, Tan P H and Eda G 2013 *ACS Nano* **7** 791
- [5] Allain A and Kis A 2014 *ACS Nano* **8** 7180
- [6] Srivastava A, Sidler M, Allain A V, Lembke D S, Kis A and Imamoglu A 2015 *Nat. Phys.* **11** 141
- [7] Wang G, Bouet L, Glazov M M, Amand T, Ivchenko E L, Palleau E, Marie X and Urbaszek B 2015 *2D Mater.* **2** 034002
- [8] Förste J, Tepliakov N V, Kruchinin S Y, Lindlau J, Funk V, Förg M, Watanabe K, Taniguchi T, Baimuratov A S and Högele A 2020 *arXiv:2002.11646* [cond-mat.mes-hall]
- [9] Rybkovskiy D V, Gerber I C and Durnev M V 2017 *Phys. Rev. B* **95** 155406
- [10] Wu Y J, Shen C, Tan Q H, Zhang J, Tan P H and Zheng H Z 2018 *Acta Phys. Sin.* **67** 147801 (in Chinese)
- [11] Koperski M, Molas M R, Arora A, Nogajewski K, Slobodeniuk A O, Faugeras C and Potemski M 2017 *Nanophotonics* **6** 1289
- [12] Liu G B, Shan W Y, Yao Y, Yao W and Xiao D 2013 *Phys. Rev. B* **88** 085433
- [13] Molas M R, Faugeras C, Slobodeniuk A O, Nogajewski K, Bartos M, Basko D M and Potemski M 2017 *2D Mater.* **4** 021003
- [14] Zhang X X, Cao T, Lu Z G, Lin Y C, Zhang F, Wang Y, Li Z, Hone J C, Robinson J A, Smirnov D, Louie S G and Heinz T F 2017 *Nat. Nanotechnol.* **12** 883
- [15] Q and Λ points in the Brillouin zone have common x, y but different z . For monolayer 2D materials, Q and Λ can be treated as the same
- [16] Lindlau J, Robert C, Funk V, Förste J, Förg M, Colombier L, Neumann A, Courtade E, Shree S, Taniguchi T, Watanabe K, Glazov M M, Marie X, Urbaszek B and Högele A 2017 *arXiv:1710.00988* [cond-mat.mes-hall]
- [17] Desai S B, Seol G, Kang J S, Fang H, Battaglia C, Kapadia R, Ager J W, Guo J and Javey A 2014 *Nano Lett.* **14** 4592
- [18] Wang Y, Cong C, Yang W, Shang J, Peimyoo N, Chen Y, Kang J, Wang J, Huang W and Yu T 2015 *Nano Res.* **8** 2562
- [19] Wickramaratne D, Zahid F and Lake R K 2014 *J. Chem. Phys.* **140** 124710
- [20] Plechinger G, Nagler P, Kraus J, Paradiso N, Strunk C, Schüller C and Korn T 2015 *Phys. Status Solidi RRL* **9** 457
- [21] Chernikov A, van der Zande A M, Hill H M, Rigosi A F, Velauthapillai A, Hone J and Heinz T F 2015 *Phys. Rev. Lett.* **115** 126802
- [22] Zhu B, Chen X and Cui X 2015 *Sci. Rep.* **5** 9218
- [23] Barbone M, Montblanch A R P, Kara D M, Palacios-Berraquero C, Cadore A R, De Fazio D, Pingault B, Mostaani E, Li H, Chen B, Watanabe K, Taniguchi T, Tonggay S, Wang G, Ferrari A C and Atatüre M 2018 *Nat. Commun.* **9** 3721
- [24] Qu F, Braganca H, Vasconcelos R, Liu F, Xie S J and Zeng H 2019 *2D Mater.* **6** 045014
- [25] Cao S, Tang J, Sun Y, Peng K, Gao Y, Zhao Y, Qian C, Sun S, Ali H, Shao Y, Wu S, Song F, Williams D A, Sheng W, Jin K and Xu X 2016 *Nano Res.* **9** 306
- [26] Chen X, Xing J, Zhu L, Zha F X, Niu Z, Guo S and Shao

- J 2016 *J. Appl. Phys.* **119** 175301
- [27] Tang J and Xu X L 2018 *Chin. Phys. B* **27** 027804
- [28] Hou H Q, Staguhn W, Takeyama S, Miura N, Segawa Y, Aoyagi Y and Namba S 1991 *Phys. Rev. B* **43** 4152
- [29] Kim S, Fisher B, Eisler H J and Bawendi M 2003 *J. Am. Chem. Soc.* **125** 11466
- [30] Kamimura H 1986 *Solid State Commun.* **59** 405
- [31] Li Y, Chernikov A, Zhang X, Rigosi A, Hill H M, van der Zande A M, Chenet D A, Shih E M, Hone J and Heinz T F 2014 *Phys. Rev. B* **90** 205422
- [32] Carvalho B R, Wang Y, Mignuzzi S, Roy D, Terrones M, Fantini C, Crespi V H, Malard L M and Pimenta M A 2017 *Nat. Commun.* **8** 1
- [33] Koperski M, Molas M R, Arora A, Nogajewski K, Bartos M, Wyzula J, Vaclavkova D, Kossacki P and Potemski M 2018 *2D Mater.* **6** 015001
- [34] Dang J, Sun S, Xie X, Yu Y, Peng K, Qian C, Wu S, Song F, Yang J, Xiao S, Yang L, Wang Y W, Rafiq M A, Wang C and Xu X 2020 *npj 2D Mater. Appl.* **4** 2
- [35] Yao W, Xiao D and Niu Q 2008 *Phys. Rev. B* **77** 235406
- [36] MacNeill D, Heikes C, Mak K F, Anderson Z, Kormanyos A, Zolyomi V, Park J and Ralph D C 2015 *Phys. Rev. Lett.* **114** 037401
- [37] Cao T, Wang G, Han W, Ye H, Zhu C, Shi J, Niu Q, Tan P, Wang E, Liu B and Feng J 2012 *Nat. Commun.* **3** 887
- [38] Nagler P, Ballottin M V, Mitioglu A A, Mooshammer F, Paradiso N, Strunk C, Huber R, Chernikov A, Christianen P C M, Schüller C and Korn T 2017 *Nat. Commun.* **8** 1551 ISSN 2041
- [39] Stier A V, McCreary K M, Jonker B T, Kono J and Crooker S A 2016 *Nat. Commun.* **7** 10643
- [40] Plechinger G, Nagler P, Arora A, Granados del Águila A, Ballottin M V, Frank T, Steinleitner P, Gmitra M, Fabian J, Christianen P C M, Bratschitsch R, Schüller C and Korn T 2016 *Nano Lett.* **16** 7899
- [41] Lyons T, Dufferwiel S, Brooks M, Withers F, Taniguchi T, Watanabe K, Novoselov K, Burkard G and Tartakovskii A 2019 *Nat. Commun.* **10** 2330
- [42] Blöchl P E 1994 *Phys. Rev. B* **50** 17953
- [43] Jain A, Ong S P, Hautier G, Chen W, Richards W D, Dacek S, Cholia S, Gunter D, Skinner D, Ceder G and Persson K A 2013 *APL Mater.* **1** 011002
- [44] Sun S, Yu Y, Dang J, Peng K, Xie X, Song F, Qian C, Wu S, Ali H, Tang J, Yang J, Xiao S, Tian S, Wang M, Shan X, Rafiq M A, Wang C and Xu X 2019 *Appl. Phys. Lett.* **114** 113104
- [45] He Y M, Clark G, Schaibley J R, He Y, Chen M C, Wei Y J, Ding X, Zhang Q, Yao W, Xu X, Lu C Y and Pan J W 2015 *Nat. Nanotechnol.* **10** 497
- [46] Srivastava A, Sidler M, Allain A V, Lembke D S, Kis A and Imamoglu A 2015 *Nat. Nanotechnol.* **10** 491